

## SMALL-ANGLE X-RAY STUDY OF DNA-DEPENDENT RNA POLYMERASE SUBUNIT $\alpha_2$ FROM *ESCHERICHIA COLI*

Otto MEISENBERGER, Ingrid PILZ and Hermann HEUMANN<sup>†</sup>

*Institut für Physikalische Chemie der Universität Graz, Heinrichstraße 28, A-8010 Graz, Austria and*

*<sup>†</sup>Max-Planck-Institut für Biochemie, 8033 Martinsried bei München, FRG*

Received 15 August 1980

### 1. Introduction

To obtain structural information about DNA-dependent RNA polymerase from *Escherichia coli* (subunit composition:  $\beta'\beta\alpha_2\sigma$ ) by small angle X-ray scattering, we are investigating the structures of these subunits of RNA polymerase which can be obtained homodispersed in solution. We proposed a structure for the  $\sigma$  subunit in [1]. Here, we report studies of the structure of the  $\alpha$  subunit, which is present in solution as a dimer  $\alpha_2$  [2,3]. The amino acid sequencing studies [4] indicate that both  $\alpha$  subunits are chemically identical and each has  $M_r$  36 500.

Few facts are available concerning the function of subunit  $\alpha$  in the transcription process [2]: One or both  $\alpha$  subunits are attached to the  $\beta$  subunit. ADP ribosylation of one  $\alpha$  subunit after infection with *E. coli* phage T4 leads to a change in the specificity of the gene expression. Our aim is to use the structural information about the isolated  $\alpha_2$  subunit in order to evaluate a model of RNA polymerase. The aim is to obtain information about the function of the subunits and their interactions.

### 2. Materials and methods

#### 2.1. Preparation of $\alpha$ subunit

The  $\alpha$  subunit was prepared from RNA polymerase as in [6]. RNA polymerase was isolated from *E. coli* as in [7] with the slight modifications in [1]. For elimination of unspecific aggregates the  $\alpha$  subunit was sedimented in a sucrose–glycerol gradient. The main fractions were pooled, concentrated by ammonium

sulfate precipitation and dialysed overnight against a buffer containing 0.05 M Tris–HCl (pH 7.5), 0.55 M  $\text{NH}_4\text{Cl}$  and  $10^{-3}$  M mercaptoethanol. This  $\alpha$  fraction reconstituted with  $\beta'$ ,  $\beta$ ,  $\sigma$  results in a fully active holoenzyme.

The purity of the  $\alpha$  subunit was >95% as checked by SDS gel electrophoresis. The homodispersity of  $\alpha$  was checked by sedimentation in an ultracentrifuge (Spinco model E). The  $\alpha$  subunit ran as a single sedimenting material with an *S*-value corresponding to the dimeric form. The concentration of  $\alpha$  factor was determined by the staining procedure developed [8], which was calibrated as in [9].

#### 2.2. Small-angle X-ray scattering

The measurements were carried out with a Kratky camera with a slit collimation system [10] using a copper tube (50 kV, 30 mA). Protein solutions were investigated at 4°C. Scattered intensities were recorded at 93 different angles from 0.00216–0.123 radians, using an entrance slit of 120  $\mu\text{m}$ . Each scattering curve was recorded several times with a fixed no. pulses ( $10^5$ )/angle in order to minimize statistical errors. The experimental arrangement and the procedures used for data evaluation were as in [1].

### 3. Results and discussion

#### 3.1. Radius of gyration and maximum dimension

Two series of measurements were performed with freshly prepared  $\alpha_2$  samples. For each sample a concentration series was measured over 6–16 mg/ml. The inner parts of the scattering curves were plotted according to Guinier ( $\log I/c$  vs  $(2\theta)^2$ ) and extrapolated to

Address correspondence to I. P.

zero concentration. This plot should yield a straight line whose slope is proportional to the square of the radius of gyration. After desmearing [11] the radius of gyration was calculated to be  $R = 4.4 \pm 0.1$  nm. This value agrees with that computed from the  $p(r)$  function [1].

The intraparticle distance distribution function  $p(r)$  was calculated with the evaluation program [11]. The function  $p(r)$  becomes zero at values of  $r$  exceeding the maximum particle dimension  $D_{\max}$ . From  $p(r)$   $D_{\max}$  results to  $15 \pm 0.5$  nm. The desmeared scattering curve of  $\alpha_2$  is shown in fig.1, and the  $p(r)$  function in fig.2.

From a plot  $Ih^2$  vs  $h^2$  (fig.3) the radius of gyration of the thickness was determined to be  $R_D = 0.64$  nm which corresponds to an averaged thickness of the particle of  $2.2 \pm 0.1$  nm [12,13]. Fig.3 shows a value of  $R_D$  which is consistent with model 1 for  $\alpha_2$ .

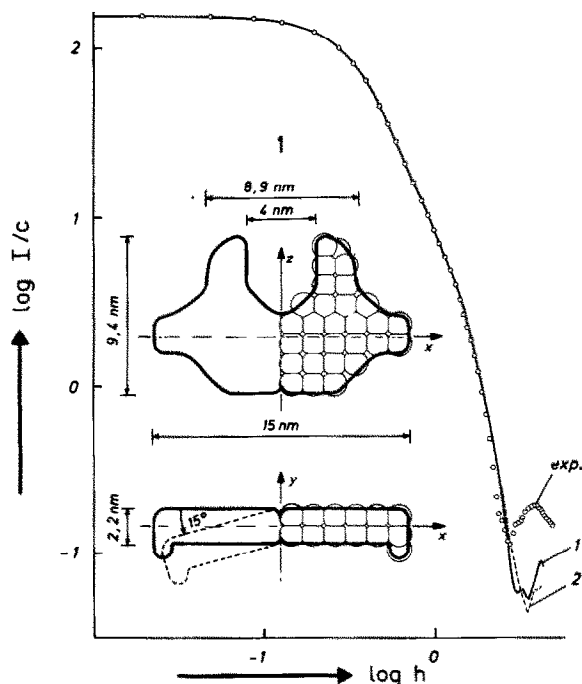


Fig.1. Comparison of the experimental scattering curve of  $\alpha_2$  ( $\circ \circ \circ$ ) with the theoretical one of model 1 (—) and model 2 (---) (see fig.2):  $I$  = scattered intensity;  $c$  = concentration;  $h = (4\pi/\lambda)\sin\theta$  ( $\lambda$  = wavelength of the  $\text{CuK}\alpha$  line,  $2\theta$  = scattering angle). Top-view and side-view of model 1. The right hand part of the picture shows the spherical subunits fit into model 1. Model calculations yielded an angle between the two  $\alpha$  components of  $180^\circ \pm 15^\circ$ . The intensities at large angles of the model scattering curve are usually lower than the experimental one, because of a lower resolution in the model.

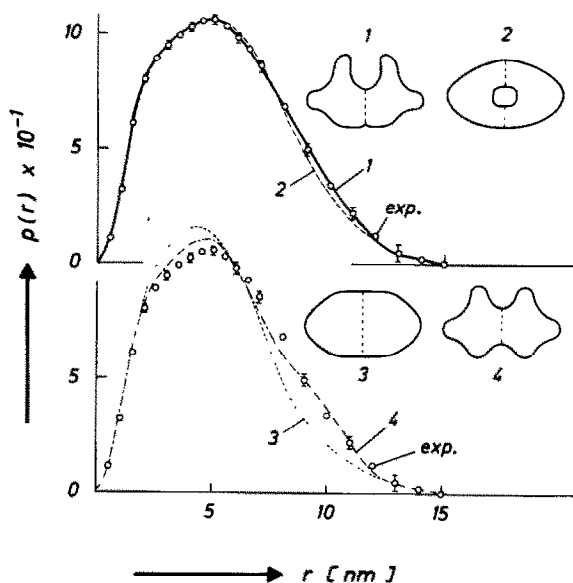


Fig.2. Comparison of the experimental distance distribution function  $p(r)$  of  $\alpha_2$  ( $\circ \circ \circ$ ) with the theoretical one of model 1 (—), model 2 (---), model 3 (..) and model 4 (-.-).  $r$  = distance;  $\hat{Q}$  = experimental data including propagated SD. The deviation of the theoretical curve of model 1 from the experimental one does not exceed the error band of the latter.

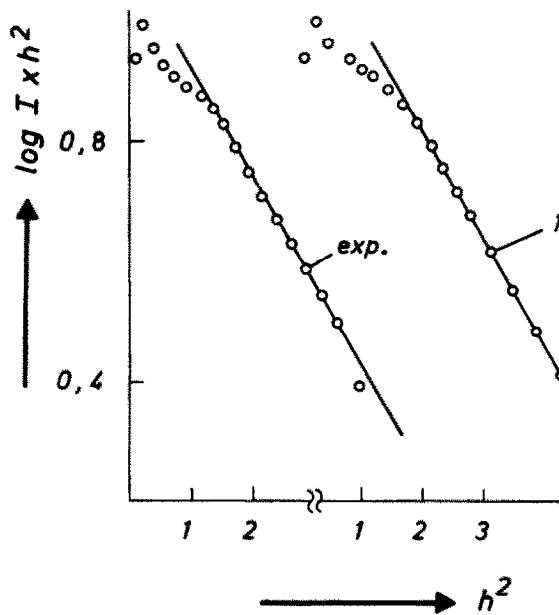


Fig.3. Plot for the determination of  $R_D$ . Comparison of the experimental curve with the theoretical one of model 1.

### 3.2. Volume

The volume of a hydrated macromolecule is proportional to its scattered intensity at zero angle and inversely proportional to its invariant  $Q$  [14]. The procedure used to determine  $Q$  is described in [1]. The volume of  $\alpha_2$  was found to be  $146 \text{ nm}^3 \pm 5\%$  by this method. Experience shows that the volume calculated from the invariant is usually affected by errors  $\geq 5\%$ , presumably due to particle inhomogeneities which come into effect at large angles.

### 3.3. Shape

Small-angle X-ray scattering allows only an indirect determination of particle shape. The most common technique is to compare the experimental scattering curve or the  $p(r)$  function with the theoretical curves of plausible models.

All model calculations were performed with a computer program which uses Debye's formula [15] to calculate the theoretical scattering curves of models composed of arbitrary spherical elements [1].

A large number of test-calculations were performed in order to find an  $\alpha_2$  model which agreed well with the experimental scattering data. Strictly speaking, model calculations can only exclude models which do not fit the experimental curve and thus produce a large number of possible solutions. To reduce this number, we had to consider the following limitations: the data of the models, such as  $R$ ,  $D_{\max}$ ,  $V$  and  $R_D$  have to be the same as those determined experimentally. Since  $\alpha_2$  is a leaf-shaped particle the shape simulation can be reduced to a two-dimensional problem. Besides there are indications that there are no structural differences between the two subunits of  $\alpha_2$  [4]. Therefore an  $\alpha_2$  model may have an approximately symmetrical shape.

The simplest model which takes into account all these facts is an elongated disc with the dimensions  $a:b:c = 15 \text{ nm}:8.5 \text{ nm}:2.2 \text{ nm}$  (model 3, fig.2). Its  $p(r)$  function clearly shows that its structure is too compact. Therefore the shape of  $\alpha$  had to be approximated by models of increasing complexity. Just as in the case of subunit  $\sigma$  (1) a lot of plausible structures were tested. For example two crevices at the  $\alpha$ - $\alpha$  binding site were calculated in a series of models (model 4, fig.2). The experimental  $p(r)$  function shows discrepancies with  $p(r)$  of all models with this structural feature.

A disc-like model with one deep crevice in the middle (probably the  $\alpha$ - $\alpha$  binding site) was found to

fit best the experimental scattering curve (model 1, fig.1) and the  $p(r)$  function (fig.2). It consists of 116 spheres each with a radius of 0.67 nm. The average thickness of 2.2 nm corresponds to two layers of model spheres.  $R_D$  determined from model 1 agrees exactly with the experimental value, as is shown in fig.3. In this plot the slope of the straight line is proportional to  $R_D^2$ . It must be mentioned that models with a hole in the centre were also in good agreement with experimental data. The best fit of models with a hole yields model 2 (fig.2) with the dimensions  $a:b:c = 15 \text{ nm}:9 \text{ nm}:2.2 \text{ nm}$  and a hole diameter of 2.4 nm. However, model 1 is in better agreement with the experimental curves. By neutron small angle scattering the radius of gyration of  $\alpha_2$  in situ in complex with the other polymerase subunits  $\beta'$ ,  $\beta$ ,  $\sigma$  was determined to be  $R = 4.7 \pm 0.2 \text{ nm}$  [16]. This  $R$ -value of  $\alpha_2$  agrees within experimental error with the  $R$ -value of isolated  $\alpha_2$ . This indicates that there are only slight structural differences between  $\alpha_2$  in the isolated state and  $\alpha_2$  incorporated in the holoenzyme.

### Acknowledgements

I. P. and O. M. thank the Österreichischen Fonds zur Förderung der wissenschaftlichen Forschung for generous support. We also thank B. Müller for drawing the figures. H. H. thanks the Deutsche Forschungsgemeinschaft for generous support of his work, Peter Stöckel for valuable discussion and Gisela Baer for excellent technical assistance.

### References

- [1] Meisenberger, O., Pilz, I. and Heumann, H. (1980) FEBS Lett. 112, 39–41.
- [2] Burgess, R. R. and Ravers, A. A. (1971) Methods Enzymol. 21D, 500.
- [3] Ho, K. and Ishiama, A. (1973) J. Mol. Biol. 79, 115.
- [4] Ovchinnikov, Yu. A. (1977) FEBS Lett. 76, 108–111.
- [5] Zillig, W., Palm, P. and Heil, A. in (1976) Subunit Function and Reconstitution in RNA-Polymerase (Losick, R. and Chamberlin, M. eds) pp. 101–125, Cold Spring Harbor Laboratory NY.
- [6] Stöckel, P., May, R., Stell, I., Cejka, Z., Hoppe, W., Heumann, H., Zillig, W., Cvespi, H., Katz, Z. Z. and Ibel, K. (1979) J. Appl. Cryst. 12, 176–185.

- [7] Zillig, W., Zechel, K. and Halbwachs, H. I. (1970) Hoppe Seyler's Z. Physiol. Chem. 351, 221–227.
- [8] Heil, A. and Zillig, W. (1970) FEBS Lett. 11, 165–172.
- [9] Heumann, H., Stöckel, P. and May, R. (1980) in preparation.
- [10] Kratky, O. (1958) Z. Elektrochem. 62, 66–73.
- [11] Glatter, O. (1977) J. Appl. Cryst. 10, 415–421.
- [12] Porod, G. (1948) Acta Phys. Austr. 2, 255–292.
- [13] Kratky, O. and Porod, G. (1948) Acta Phys. Austr. 2, 133–147.
- [14] Porod, G. (1951) Kolloid Z. 124, 83–114.
- [15] Glatter, O. (1972) Acta Phys. Austr. 36, 307–315.
- [16] Stöckel, P., May, R., Strell, I., Cejka, Z., Hoppe, W., Heumann, H., Zillig, W. and Crespi H. L. (1980) submitted.